LASER DRIVEN DIELECTRIC ACCELERATOR IN THE NON-RELATIVISTIC ENERGY REGION *

Kazuyoshi Koyama†, Mitsuru Uesaka, The University of Tokyo, Tokai, Ibaraki, Japan
Mitsuhiro Yoshida, KEK, Tsukuba, Ibaraki, Japan
Sunao Kurimura, NIMS, Tsukuba, Ibaraki, Japan
Hayato Okamoto, Shohei Otsuki, The University of Tokyo, Tokyo, Japan

Abstract

Laser-driven dielectric accelerator (LDA) is suitable for delivering a submicron-size ultra-short electron beam, which is useful for studying basic processes of the radiation effect in a biological cell. Both the oblique incidence and the normal incidence configurations of LDA were studied. The oblique incidence configuration of LDA relaxes the synchronization condition as $v_e = \pm cL_G/(\lambda + L_G n \sin\theta)$ and is somewhat suitable for accelerating the non-relativistic electrons. The required energy to accelerate electrons in the oblique incidence configuration is smaller than that in the normal incidence configuration by a factor of $\cos\theta$, where θ is the incidence angle of the laser beam. Two gratings each were made of different material structure of silica (SiO_2) were fabricated by the electron beam lithography. When a crystal silica was adopted, many large humps of several hundred nm size were observed in grooves of the grating. On the other hand, a glass silica had smoother grooves.

INTRODUCTION

In order to estimate the health risk associated with a low radiation dose, basic radiobiological processes must be clarified by shooting at a DNA by using a spatially and temporally defined beam of ionization radiation. The suitable beam size is as small as a resolving power of an optical microscope of sub-micron. The required beam energy and bunch charge are in the range from 0.5MeV to 1MeV and from 0.01fC to 1fC, respectively [4]. Moreover, a laser-driven dielectric accelerator (LDA) which can be handled under the optical microscope is a suitable device for delivering the sub-micron beam.

An acceleration field of the LDA is produced by modulating a wavefront of a laser beam by a properly designed dielectric structure such as a binary blazed grating. The first idea of the accelerator with use of proximity field of the reflection grating was published in 1968 [1]. Demonstration experiments of LDA were performed by using transmission gratings (TRGs) at SLAC and MPQ and published in 2013 [2] [3]. However, there are many problems to be solved before designing the laser-driven on-chip accelerator, especially in the non-relativistic energy region. We report on the oblique incidence configuration as well as the normal incidence configuration of LDA and fabrication of the TRG.

* Work supported by KAKENHI, (Grant-in-Aid for Scientific Research) Grant Number 15H03595
† koyama@nuclear.jp

CONFIGURATION OF LDA

Normal Incidence

The TRG is defined by the grating constant L_G, the width of grating pillar L_P, the height of the pillar H_P, and the length of the pillar W as illustrated in Fig.1. If a pair of gratings are used to make an acceleration channel, the gap distance between two gratings D must be considered. A distribution of the electric field is similar to a standing wave, which is orthogonal to the pillars in the proximity of the grating surface. The standing wave is expressed by superposition of two counter propagating waves, whose phase velocity are $v_{ph} = \pm cL_G/\lambda$ at a normal incidence to the grating, where v_e, c, L_G and λ are the speed of the electron, the speed of light in a vacuum, the grating constant and the laser wavelength, respectively. If the electrons velocity is slightly slower than one of phase velocities v_{ph}, the electrons are trapped in a wave potential and accelerated the phase velocity of the wave.

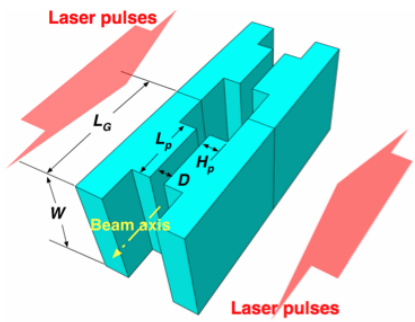

Figure 1: Schematic drawing of two periods of an accelerator unit.

Optimal geometry of TRG is analytically defined as $(L_G/N)/\lambda = v_e/c$, $L_P/L_G \approx 0.5$, $H_P/\lambda = 1/2(n-1)$, $D/\lambda \leq (L_P/\lambda)/2 = L_G/(2\lambda)2 \approx 1/4$, where $N = 1, 2, 3, \cdots$ is a mode number of the Fourier series of the grating surface. In order to accelerate the non-relativistic electron in the normal incidence configuration, we must adopt a shorter grating constant or higher order harmonics of the grating period, because the synchronization condition of $v_{ph} \approx v_e$ must be fulfilled. If it is difficult to fabricate a high aspect ratio grating of $H_P/(L_G - L_P) \geq 2$, the moderate aspect ratio of $H_P/(L_G - L_P) \approx 1$ is the next best solution. However, the energy gain is decreased to half of the optimal condition, because the pillar hight is as short

ISBN 978-3-95450-147-2

as $H_P/\lambda = 0.6$ at the moderate aspect ratio. An estimation of the acceleration gradient at various parameters was discussed based on results of the finite-difference time-domain (FDTD) simulation [4].

Oblique Incidence

Another method for accelerating the non-relativistic electron is to slow the phase velocity of one component of the standing wave. When the laser beam arrives at the surface of the TRG with the incidence angle of θ, the tangential component of the propagation velocity of the laser beam of $v_{||} = c/(n\sin\theta)$ changes the propagation velocity of the acceleration waves from v_{ph} to $v_{obl} = \pm cL_G/(\lambda + L_G n\sin\theta)$, where n is the refractive index of the grating material. We can therefore conclude that the oblique incidence configuration moderately relax the synchronization condition as shown in Fig. 2 [5]. It is possible to produce the standing-wavelike longitudinal electric field near the TRG even though in the oblique incidence configuration as shown in Fig. 3.

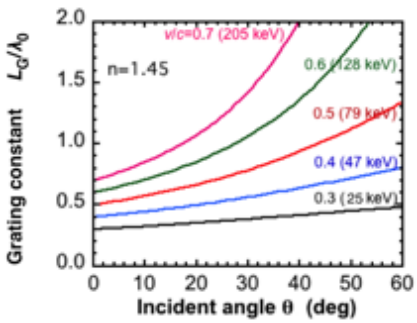

Figure 2: Grating constants for satisfying the synchronization condition in the oblique incidence configuration.

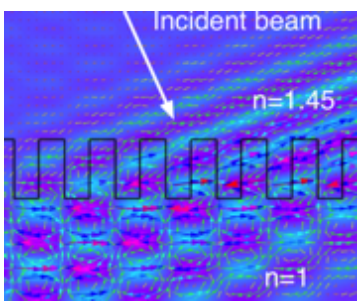

Figure 3: The snapshot of the electric field distribution. The pseudo color map indicate the horizontal component of the field. Arrows show the electric field vector.

Since the laser beam must irradiate whole acceleration length of $X_{ac} = v_e\tau_L$, the length and the width of the rectangular shape of the laser beam is $D_L = X_{ac}\cos\theta = v_e\tau_L\cos\theta$ and w, where τ_L is the pulse width of the laser. The required laser energy for the oblique incidence configuration is derived to be

$$W_L = \frac{1}{2}\varepsilon_0\frac{\Delta E_{ac}^2}{e^2}w\cos\theta\left(\frac{\lambda}{L_G} + n\sin\theta\right), \qquad (1)$$

where E_{ac}, ε_0 and e are the acceleration electric field proportional to the laser electric field, the permittivity of vacuum and the electron charge, respectively. Equation (1) is expressed as $W_L \propto \cos\theta\,(c/v)$ by using the synchronization relation., that is to say, the required energy for the oblique incidence acceleration is smaller than that of the normal incidence acceleration by a factor of $\cos\theta$.

FABRICATION OF LDA

Accuracy for Processing and Assembling

A required processing accuracy was numerically evaluated for the case of the relativistic electron acceleration, i.e. $L_G/\lambda = 1$. An normalized acceleration gradient (average acceleration field) E_x/E_0 varies with a filling factor of the grating L_P/L_G as shown in Fig. 4(a), where E_x and E_0 are the acceleration gradient and the incoming laser field strength, respectively. When the filling factor of the pillar is within a range of $0.47 \le L_P/L_G \le 0.58$, a decline of the acceleration gradient from the optimum value remains smaller than $\Delta E_x/E_x/ \le 5\%$. The height of the pillar must be remained in the range of $0.89 \le H_P/\lambda \le 0.99$ for keeping $\Delta E_x/E_x/ \le 5\%$ (Fig. 4(b)). The influence of the deviation angle from the vertical wall of the grating pillar $\Delta\theta$ on E_x/E_0 is shown in Fig. 4(c), where the filling factor at the top of the pillar is assumed to be $L_P/L_G = 0.5$. In order to set a decrease of the acceleration gradient to $\Delta E_x/E_x \le 5\%$, the deviation angle from the vertical must be $-2^\circ \le \Delta\theta \le 3^\circ$ (the inclination $\theta \ge 88^\circ$).

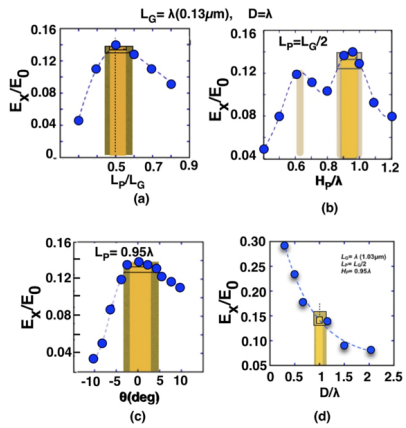

Figure 4: The changes of the acceleration gradient as functions of the filling factor L_P/L_G (a), the hight of the pillar H_P/λ (b), the angle of inclination of the side wall of the pillar $\Delta\theta$ (c), and the gap distance D (d).

The acceleration gradient exponentially decreases according as the gap distance between two gratings D increases as shown in Fig. 4(d). An extremely small fluctuation of the gap distance of $\Delta D/\lambda \le \pm 1/80$ is allowed to keep $\Delta E_x/E_x/ \le 5\%$ at the gap distance of $D/\lambda = 1/4$; however, the restriction becomes moderate as $\Delta D/\lambda \le \pm 1/20$ at the wider gap distance of $D/\lambda = 1$.

Trial Fabrication of TRG

We tried to fabricate the high aspect ratio TRG in order to check a fabrication process, accuracy, etc. An electron beam lithography technique is applied to process a silica (SiO_2) . Design parameters of the grating were L_G = 560nm, L_P = 280nm and H_P = 440nm. The etching rate of $y = 0.911t - 29.9$ was measured for a crystal quartz at NIMS in advance, where y and t were the etched depth (nm) and etching time (s), respectively. Two different material structures of silica, the crystal quartz and a glass silica, were processed with same etching conditions. The grating constant and the pillar width measured by using the variable pressure scanning electron microscope (VP-SEM) were L_G = 550nm and L_P = 238nm, respectively, as shown in Fig. 5.

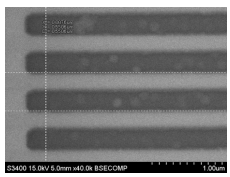

Figure 5: The SEM image of the transmission grating.

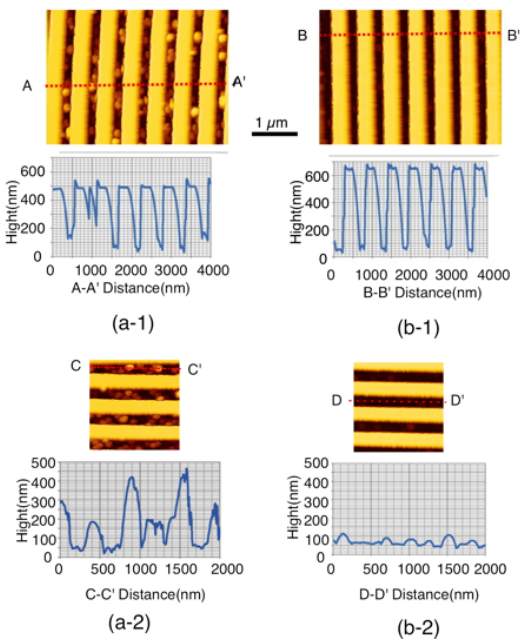

Figure 6: AFM images with sectional shapes along red dotted lines of TRGs. (a-1) and (a-2) are the AFM images of crystal quartz TRG. (b-1) and (b-2) are that of the glass silica TRG.

The groove depth measured by an atomic force microscope (AFM) were 421nm and 583nm for the crystal quartz and the silica glass, respectively. The SEM image and the AFM images show many humps at the bottom of the groove of the TRG made of the crystal silica. The typical diameter and height of the hump were in the range of 100nm - 300nm and 140nm - 400nm, respectively (Fig. 6 (a-2)). On the other hand, the sparse and smaller humps were seen in the groove of glass silica TRG. The size was as small as 20nm -50nm (Fig. 6 (b-2)).

It is difficult to know the exact inclination of the side wall of the pillar due to the shape of the cantilever of the AFM. From the cross sectional shape measured by the AFM, we can conclude that the inclination of the pillar wall is steeper than 82° as seen in Fig. 6 (a-1) and (b-1).

From results of the test fabrication, we conclude that the glass silica is more suitable for making the TRG and the fabrication of the high aspect ratio grating of ≈ 1.9 was possible.

SUMMARY

Both the oblique incidence and the normal incidence configurations of the LDA were studied. The oblique incidence configuration relaxes the synchronization condition as $v_{obl} = \pm cL_G/(\lambda + L_G n \sin\theta)$. The oblique incidence configuration is therefore rather suitable for accelerating the non-relativistic electrons. The required laser energy for the oblique incidence acceleration is smaller than that for the normal incidence acceleration by a factor of $\cos\theta$, where θ is the incidence angle of the laser beam.

Two gratings were fabricated on two different material structure of silica by the electron beam lithography. The large humps of several hundred nm size were observed in grooves of the TRG made of the crystal silica. On the other hand, a glass silica TRG had smoother grooves. the glass silica is more suitable for making the TRG and the fabrication of the high aspect ratio grating of ≈ 1.9 was possible.

ACKNOWLEDGMENT

Authors would like to express our gratitude to Dr. Onose of Hitachi High-Technology Co.. This work was supported by KAKENHI, Grant-in-Aid for Scientific Research (B)15H03595.

REFERENCES

[1] K. Koyama *et al.*, in *J. Phys. B: At. Mol. Opt. Phys.*, vol. 47, p. 234005, 2014.

[2] T. Takeda and I. Matsui, in *Nucl. Instrum. Methods*, vol. 62, p. 305, 1968.

[3] E. A. Peralta *et al.*, in *Nature*, vol. 503, p. 91, 2013.

[4] J. Breuer and P. Hommelhoff, in *Phys. Rev. Lett.*, vol. 111, p. 134803, 2013.

[5] S. Otsuki *et al.*, in *Proc. of IPAC'14*, Dresden, Germany, paper TUPME037, p. 1434.

ISBN 978-3-95450-147-2